3D MODELING OF DYNAMIC RUPTURE PROPAGATION BASED ON A BOUNDARY INTEGRAL EQUATION METHOD FOR EARTHQUAKES IN CHINA

Zhang Lifen[*] **Supervisor:** **Taku Tada**[**]
MEE10501 **Bunichiro Shibazaki**[***]

ABSTRACT

We developed a code for dynamic rupture propagation on arbitrarily shaped faults based on the stress Green's function corresponding to a triangular mesh fault element. A boundary integral equation method is adopted in this study. Starting from representative theorem, after regularization and descretization of a basic elastodynamic equation relating stress with slip, a more applicable formulation used in dynamic rupture simulation is constructed. For a boundary condition, we utilize a simple but typical slip weakening friction law. In order to avoid numerical oscillation, according to Courant-Friedrichs-Lewy (CFL) condition, time intervals used in the simulation is given as $\Delta t \leq \sqrt{2}l/6C_L$ (l is the element size, and C_L denotes P wave velocity). And then we applied the code to a planar fault and a curved fault.

For a simple planar fault, spontaneous rupture propagation initiates from a given circular asperity and then propagates symmetrically and bilaterally around the central point. A bump of slip distribution near the center of the fault is the most characteristic feature of the fault that starts from a finite asperity. In addition, we considered a curved fault with different final inclination angles. The curved fault with a small inclination angle does not have significant effects on the rupture propagation. The rupture still can expand symmetrically and bilaterally beyond a bend. However, a large inclination angle may cause the rupture to propagate asymmetrically. Initial conditions determine the rupture propagation behavior. Given the same initial stress on the same fault, the smaller the critical slip weakening displacement is, the faster and longer the rupture propagates. Initial stresses inside and outside of the asperity (T_{asp}, T_e) also have great effects on the rupture propagation. If T_e is too small, the rupture will stop soon after initiation. If T_e becomes larger, the rupture can propagate longer and faster with subshear velocity.

Keywords: Boundary integral equation method, Triangular fault mesh, Dynamic rupture propagation, Slip weakening friction law

1. INTRODUCTION

It has often been observed that earthquake rupture propagates along pre-existing faults with complex geometry in the continental crust. These fault complexities, sometimes referred to as nonplanar faults, include fault bending, jogs, step-overs, branches and so on. In order to understand how these complex fault geometries affect the rupture propagation, dynamic numerical simulation provides insight into physical effects of nonplanar fault geometry on the earthquake rupture and slip process. In addition, a

[*]Earthquake Administration of Hubei Province, China.
[**] Asahi Shimbun General Service, Japan.
[***]Building Research Institute, Japan.

physical understanding of the earthquake rupture process can improve our capability for predicting ground motion, and therefore our assessment of seismic hazard (Duan and Oglesby, 2005).

Many numerical methods have been used for dynamic simulation. Finite difference method (FDM) and finite element method (FEM) are so-called field domain methods, which are applicable to arbitrary geologic structures and fault geometries, but require a field discretization within the domain of interest (Goto and Bielak, 2008). In contrast, boundary integral equation method (BIEM) is more powerful, which is a boundary based method. Because a problem is solved not in the whole volume but only on the fault surfaces, it simplifies the problem and requires small resources in computation. In addition, for fault rupture problem, it is easy to consider the singularity at the tip of crack using BIEM. Therefore, in the present paper, we adopt this method to describe the dynamics of 3-D cracks with arbitrary geometry. Compared with rectangle meshes, triangle meshes are more appropriate to describe the complex fault geometry. However, few researchers model the dynamic rupture propagation using Green's function calculated with triangular fault meshes. Therefore, in the present study, we will develop a code to do the 3-D dynamic rupture simulation using triangular fault meshes.

2. THEORY AND METHODOLOGY

2.1. Boundary Integral Equation Method

Boundary integral equation starts from representative theorem (Aki and Richards, 1980), which states the relationship between displacement at receiver location and slip across a fault. However, for a dynamic problem, stress should be taken into consideration. Based on this theorem, a basic elastodynamic equation relating stress with slip is constructed. For the 3-D case, slip is assumed to occur along the x_1- and x_2-axis, so the stress along the x_1- and x_2-axis can be represented as:

$$\mathrm{T_1(x,t)} = \mathrm{T_1^0} - \mu^2 \int_{\Gamma} \mathrm{dS}(\xi) \int_0^t \mathrm{d}\tau \left[\Delta \mathrm{u_1}(\xi,\tau) \left(\frac{\partial^2}{\partial \mathrm{x_3^2}} \mathrm{G_{11}} + 2 \frac{\partial^2}{\partial \mathrm{x_1}\, \partial \mathrm{x_3}} \mathrm{G_{13}} + \frac{\partial^2}{\partial \mathrm{x_1^2}} \mathrm{G_{33}} \right) + \Delta \mathrm{u_2}(\xi,\tau) \left(\frac{\partial^2}{\partial \mathrm{x_3^2}} \mathrm{G_{12}} + \frac{\partial^2}{\partial \mathrm{x_2}\, \partial \mathrm{x_3}} \mathrm{G_{13}} + \frac{\partial^2}{\partial \mathrm{x_1}\, \partial \mathrm{x_3}} \mathrm{G_{23}} + \frac{\partial^2}{\partial \mathrm{x_1}\, \partial \mathrm{x_2}} \mathrm{G_{33}} \right) \right] \tag{1}$$

where G_{ij} denotes Green's function, $\Delta u_1(\xi,\tau)$ and $\Delta u_2(\xi,\tau)$ denotes the slip along the x_1- and x_2-axis, μ is the rigidity, Γ is the fault surface, T_1^0 is the initial stress along x_1-axis. And $T_2(x, t)$ has symmetrical form with $T_1(x, t)$.

2.2. Regularization and Discretization

The traction boundary integral equations, thus derived, are hypersingular, and cannot be directly used in numerical modeling. Tada et al. (2000) solved this difficulty by enlarging Fukuyama and Madariaga's (1998) integration by parts technique to derive a non-hypersingular time-domain boundary integral equation for the 3-D non-planar crack in a fully explicit form. However, the boundary equation is still too abstract to be utilized in numerical simulation. Therefore, discretization is needed. When discretizing the fault surface, in general, the size of the mesh elements may be either homogeneous or variable along the fault, but the time step intervals are usually taken to be homogeneous. Additionally, based on collocation method and piecewise constant approximation method, the boundary integral equation can be discretized to be a more applicable form (Eq. (2)). For the simulation, we put receiver at the collocation point of each element. And the time collocation point had better be put at the end point of each time intervals.

$$T_{mp} = T_0^m + \sum_{n=1}^{N_X} \sum_{p=1}^{p} V_{nq} \int_{\Gamma} dS(\xi) \int_0^t d\tau\, \hat{K}(x_m, t_p - \tau; \xi, 0) \mathrm{H}(\xi \in \Gamma_n) \left[\mathrm{H}(\tau - t_{q-1}) - \mathrm{H}(\tau - t_q) \right] \tag{2}$$

where V_{nq} is the discrete slip rate, $H(\xi \in \Gamma_n)$ and $H(\tau - t_{q-1}) - H(\tau - t_q)$ denote that if slip occurs within Γ_n during a certain time intervals, slip rate is unity, otherwise it is zero. $\widehat{K}$ is the integration kernel, which is a response function. During the simulation, the calculation of the kernel is of great importance.

2.3. Numerical Stabilization

An exponentially growing numerical oscillation in BIEM is well known in the BIEM community (Tada and Madariaga, 2001). It has been recognized that the oscillation is coming from the spatiotemporal discretization, therefore, an appropriate and optimum combination of space grid and time intervals is very important, which can suppress the stability to some extent. We adopt the common method of Courant-Fridrichs-Lewy condition. Due to the triangular fault meshes, the time interval (Δt) is chosen as $\Delta t \leq \sqrt{2}l/6C_L$ (l denotes the element size, and C_L denotes the P wave velocity).

3. DATA AND VALIDATION

3.1. Coordinate Transform

For the planar fault, we can describe its geometry just using global Cartesian coordinate system. However, it is a little difficult to define the nonplanar fault. Instead, Tada (2009) solved this difficulty by making use of a local Cartesian coordinate system.

We assume that slip occurs on a triangular fault element, with its vertices named A, B and C, which is embedded in a 3D infinite, homogeneous and isotropic medium. For convenience, the local coordinate system is defined according to the following rules:

(1) The system of local Cartesian coordinates (x_1, x_2, x_3) is right handed, and shares the origin with the system of global Cartesian coordinates (X_1, X_2, X_3), which is also right handed.

(2) The x_3-axis is perpendicular to the fault element and the direction is upward. Vertices A, B and C are aligned counter-clockwise in this order when seen in the $+x_3$-direction.

(3) The x_1-axis can be defined in any arbitrary direction as long as it is normal to the x_3-axis, but in our case, we define it parallel to the slip direction on the fault. Totally, there are five coordinate systems used to calculate the stress Green's function.

3.2. Validation for the Green's function

After obtaining the corresponding local coordinates, to validate the accuracy of the stress computation, we calculated the different components of the Green's function $L_{ij/k}$ caused by a constant slip rate of unit magnitude taking place in the x_k-direction across triangles ABC or CDA at receiver location R(0.6,0.3,0.2). By comparison with Tada (2006), as shown in Figure 1, our results are in very good agreements. In this validation, triangular faults ABC and CDA, with vertices located at A(0,0,0), B(1,0,0),C(1,1,0) and D(0,1,0) in the local $x_1x_2x_3$-coordinate system. The shear wave velocity is 1.0 km/s, and the P wave velocity is 1.73 km/s.

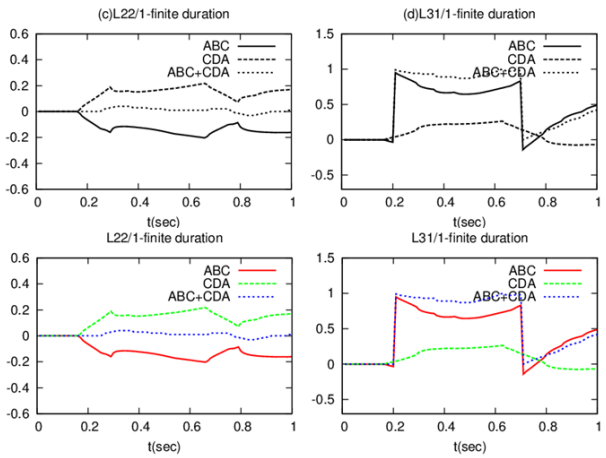

Figure 1. Comparison of the different components of Green's function computed using the 3-D kernels of BIEM by this study (the lower figures) and Tada (2006) (the upper figures).

4. RESULTS AND DISCUSSION

For dynamic rupture simulation, we need to evaluate slip, slip velocity and stress. As a boundary condition, we adopt simple but typical slip weakening friction law. We apply the code to a planar and a nonplanar fault with different inclination angles.

4.1. Planar and Nonplanar Fault Model

Table 1. Parameters used in dynamic simulation

Dimension(km)	Δx(km)	Nx	Δt(sec)	Nt
21 × 10	1.0	600	0.045	200
D_c (m)	T_p (MPa)	T_{asp}(MPa)	T_e(MPa)	μ(MPa)
0.08	1.0	1.2	0.8	30,000

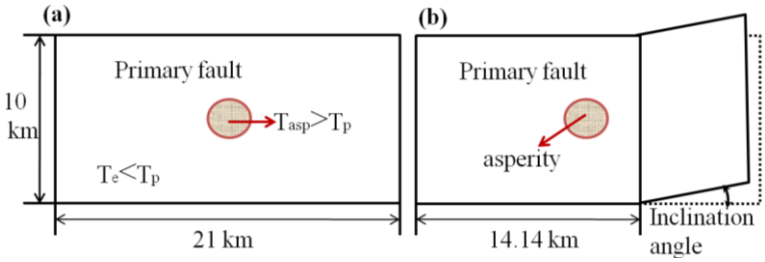

Figure 2. Schematic fault geometries of a planar and a nonplanar fault. T_{asp} and T_e denote the stress inside and outside of the asperity. T_p is the peak strength. Figure 2(a) and Figure 2 (b) show the planar and nonplanar fault model.

The fault geometries of planar and nonplanar fault are shown in Figure 2. It is well known that in order to initiate rupture in such a model, an initial high stress patch must be ready to break (Andrews, 1976).

We study spontaneous rupture of a fault starting from a circular asperity that is ready to break. It is loaded with stress that is larger than the peak strength and surrounded by a bounded fault surface where the initial stress is smaller than the peak strength. The parameters are listed in Table 1. In this table, the mesh size is chosen as 1.0 km, and considering the numerical stability, the time intervals is 0.045 second.

4.2. Rupture Propagation on a Planar Fault

For a planar fault, the rupture initiates from the circular asperity and then propagates symmetrically and bilaterally. Figure 3 shows the slip distributions on the fault plane as a function of time and position along the *x* axis of the fault. We can observe the rupture starts from the localized asperity around the center of the fault and then grows bilaterally at a slightly increasing slip rate. Comparing my result with Madariaga et al. (1998), we can find the consistence of a bump at the center of the fault. This localized excess slip is the most characteristic feature of faults that start from a finite asperity, which is common phenomenon for most slip functions (Madariaga et al. 1998). However, if the initial radius of asperity is too small, the bump is insignificant.

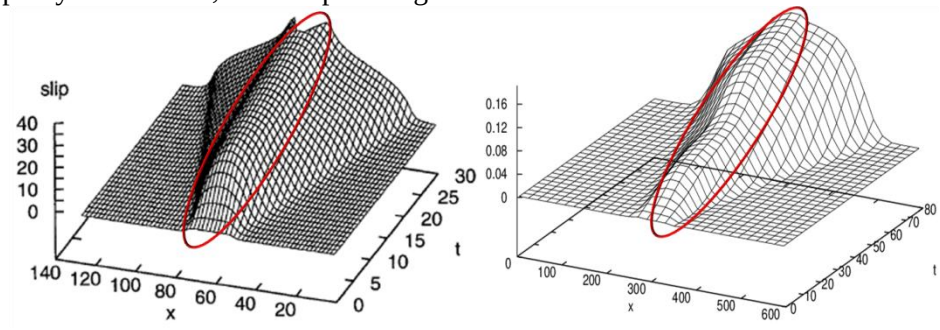

Figure 3. Comparison of spontaneous slip of the bounded rectangular fault.
(Left -Madariaga et al (1998), Right -Present study)

4.3. Rupture Propagation on a Nonplanar Fault

For a nonplanar fault, the bending position is put at x=14.14 km, and we consider two cases with different inclination angles of 10˚ and 30˚. The series of snapshots in Figure 4 (a) and Figure 4(b) show the evolution of slip velocity for curved fault model.

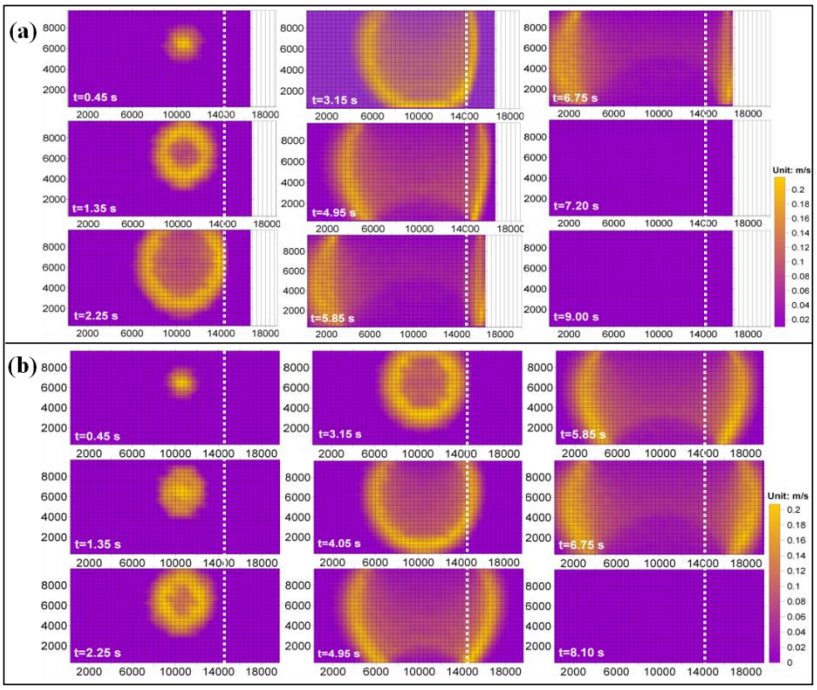

Figure 4. Snapshots of slip velocity for the nonplanar fault with inclination angle of 10˚ and 30˚. (Unit of horizontal and vertical axis: km)

For both cases, the ruptures expand symmetrically on the primary fault until the rupture front reach the bend. In the case of the small bend with the final inclination angle of 10˚ (Figure 4(a)), the rupture can propagate symmetrically beyond the bend, which is similar with planar fault rupture propagation. When the final inclination angle increases to 30˚ (Figure 4(b)), at 2.25 seconds, the rupture front reaches the bending boundary of the fault. However, the rupture cannot propagate symmetrically any more beyond the bend. It illustrates that curvature fault with big final inclination angle hinders the rupture propagation, which behaves like a barrier to some extent.

4.4. Influence of Initial Conditions on Rupture Propagation

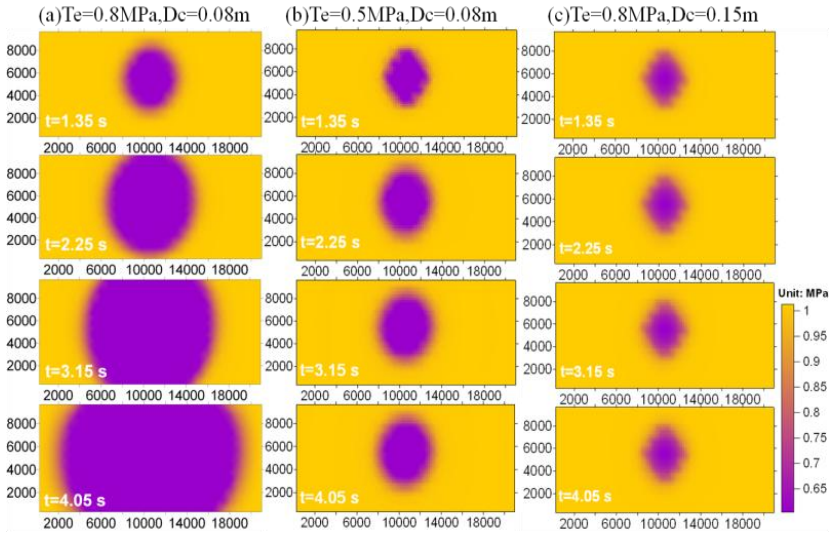

Figure 5. Snapshots of stress for the different initial conditions on the rupture propagation. (Unit of horizontal and vertical axis: km)

In the simulation, we give different initial conditions to examine their effects on the rupture propagation. When the initial stresses inside and outside of the asperity are given, it is easy to find that the smaller the slip weakening displacement (D_c) is, the faster and longer the rupture propagates (Figure 5(a)). If D_c is too large, the rupture easily terminates (Figure 5(c)). Another important factor is the stress outside of the asperity (T_e), by comparison, it is illustrated that small T_e easily causes the rupture to stop (Figure 5(b)).

5. CONCLUSIONS

The purpose of this study is to simulate the complex fault dynamic rupture propagation based on the boundary integral equation method. In order to attain the goal, we developed a code and validated it. We applied the code to the spontaneous rupture on a rectangular planar fault and curved fault in an infinite homogeneous medium, starting from a circular asperity under the slip weakening friction criterion. By analyzing the different cases, we had some findings.

For the planar rectangular fault with homogeneous initial stress field, the rupture initiates from the circular asperity and then propagates symmetrically and bilaterally. The bump of the slip distribution (excessive slip) near the center of the fault is the most characteristic feature of the fault that starts from a finite asperity.

For the curved rectangular fault with different inclination angles, the small bend angle does not have great influence on the rupture propagation. Instead, the large bend angle may behave like a barrier.

The initial conditions have great influences on the rupture propagation. Given the same initial stress on the same fault, critical slip weakening displacement (D_c) determines the rupture propagation. The smaller the D_c is, the faster and longer the rupture propagates. The initial stresses inside and outside of the asperity (T_{asp}, T_e) also have great effects on the rupture propagation. If the T_e is too small, the rupture will stop soon after initiation. If the T_e becomes larger, the rupture can propagate longer and faster with sub-shear velocity.

6. RECOMMENDATION

The boundary integral equation method is good at dealing with nonplanar fault problems. However, it has only limited applicability to a full space and a homogeneous medium. But for real earthquake researches, the free surface has some effects on the rupture propagation. In addition, for the dynamic simulation, it takes much time and computer memory. Therefore, according to above limitations, we recommend the following suggestions:

i. In order to compensate the weakness of boundary integral equation method, it is essential to resort to the advantages of other numerical methods. For the strike-slip faults, we can resort to the imaginary mirror sources to consider the influence of free surface. For other faulting types, we also should find the solutions.
ii. More appropriate algorithm and flexible program are required for modeling dynamic rupture propagation.

REFERENCES

Aki, K. and Richards, P.G., 1980, W.H. Freeman, San Francisco.
Andrews, D. J., 1976, J. Geophys. Res., 81, 5679-5687.
Duan, B,C. and Oglesby, David D., 2005, J. Geophys. Res., 110, B03304
Fukuyama, E., and Madariaga, R., 1998, Bull. Seism. Soc.Am. 88, 1-17.
Goto, H., and Bielak, J., 2008, Geophys. J Int., 172, 1083-1103.
Madariaga, R., Olsen, K., and Archuleta, R., 1998, Bull. Seism. Soc. Am. 88, 1182-1197.
Tada, T., Fukuyama, E., and Madariaga, R., 2000, Computational Mechanics, 25, 613-626.
Tada, T., 2006, Geophysical Journal International, 653-669
Tada, T., 2009, International Geophysics, Elsevier Inc , USA.